Functional Roles of Ionic and Hydrophobic Surface Loops in Smooth Muscle Myosin: Their Interactions with Actin†

Shin-ichiro Kojima,‡ Kaoru Konishi,‡,§ Kazuo Katoh,‡ Keigi Fujiwara,‡ Hugo M. Martinez,|| Manuel F. Morales,⊥ and Hirofumi Onishi*,‡

Department of Structural Analysis, National Cardiovascular Center Research Institute, Fujishiro-dai, Suita, Osaka 565-8565, Japan, Division of Chemistry, Graduate School of Science, Hokkaido University, Sapporo, Hokkaido 060-0810, Japan, University of California, San Francisco, California 94143, and University of the Pacific, San Francisco, California 94115

Received May 18, 2000; Revised Manuscript Received September 19, 2000

ABSTRACT: This investigation ascertains whether, in (smooth muscle) myosin, certain residues engage in functional interactions with their actin conjugates in an actomyosin complex. Such interactions have been postulated from putting together crystallographic models of the two proteins [Rayment, I., Rypniewski, W. R., Schmidt-Bäse, K., Smith, R., Tomchick, D. R., Benning, M. M., Winkelmann, D. A., Wesenberg, G., and Holden, H. M. (1993) *Science 261*, 50−58]. Here, in several instances, we ask whether mutation of a particular residue significantly impairs a function, and find that the answers are largely rationalized by the original postulation. Additionally, a novel element emerges from our investigation. To assess function, we test the wild type and mutant systems as they perform in the steady state of ATP degradation. In doing so, we assume, as usual, that degradation proceeds from an early stage in which the complex forms (and is described by parameter K_{app}) to a later stage during which the product leaves the complex (and is described by parameter V_{max}). Interestingly, certain defects induced by the mutations are associated with changes in K_{app}, and other defects are associated with changes in V_{max}, suggesting that our procedure at least roughly distinguishes between events according to the time in the degradation at which they occur. In this framework, we suggest that (1) in the actin−myosin association phase, cationic residues Lys-576 and Lys-578 interact with anionic residues of the so-called second actin, and (2) in the product leaving phase, hydrophobic residues Trp-546, Phe-547, and Pro-548, as well as the Thr-532/Asn-533/Pro-534/Pro-535 sequence, sever connections with the so-called first actin. The role of Glu-473 is also examined.

After it had been learned that myosin and actin are partners in the contractile interaction, it is natural to ask, at what points do they touch? A first answer was given by Rayment et al. (*1*, *2*). By putting together their crystallographic models, they suggested many likely contacts. On the myosin side, they suggested as contacts a positively charged surface loop issuing from the 50 kDa−20 kDa junction (that might interact with the negatively charged N-terminus of the "first actin"), and the small, lysine-rich positively charged loop (that might interact with the Glu-99/Glu-100 sequence of the "second actin"). They also suggested several potential actin-binding "hydrophobic" residues near the 50 kDa−20 kDa loop. From their suggestions and by appealing to homology, we assume that in smooth muscle myosin, Lys-576 and Lys-578 constitute the small loop and may bind the second actin. An inference of our own is that Glu-473, though not in the loop, may be close enough to modify the interaction with actin. Also, there are two hydrophobic surface loops which, from homology with skeletal muscle myosin, may bind actin (*1*, *2*). One is the Trp-546/Phe-547/Pro-548 triplet; another is the Thr-532/Asn-533/Pro-534/Pro-535 loop. These potential sites of interaction with actin, as inferred from crystallography, are noted in Figure 1.

An aim of this paper is to examine whether the contacts so inferred are correct. Site-directed mutation enables the replacement of one partner in a presumed contact, and thus the testing of whether a particular replacement makes a functional difference in the behavior of the system. Testing requires formulation of a time-dependent model to which parameters are assigned from observation. Comparing the values assigned to the wild-type system with those assigned to the mutant system then determines whether the examination agrees with the crystallographic inference. If the parameters are different, then the functional test confirms the inference; if they are the same, one concludes that the inference is uncertain (a contact may or may not occur, but if it does, it is not significant for the behavior of the system).

† This work was supported by Research Grants for Cardiovascular Diseases from the Ministry of Health and Welfare of Japan, by Grants-in-Aid for Scientific Research from the Ministry of Education, Science and Culture of Japan, by Special Coordination Funds for Promoting Science and Technology from the Science and Technology Agency of Japan (to H.O. and K.F.), and by Grant MCB 9603670 from the National Science Foundation (to M.F.M.). S.-i.K. is a recipient of the Domestic Research Fellowship from the Japan Science and Technology Corp.

* To whom correspondence should be addressed. Telephone: +81-6-6833-5012. Fax: +81-6-6872-8092. E-mail: honishi@ri.ncvc.go.jp.

‡ National Cardiovascular Center Research Institute.

§ Hokkaido University.

|| University of California.

⊥ University of the Pacific.

10.1021/bi0011328 CCC: $20.00
Published on Web 12/22/2000

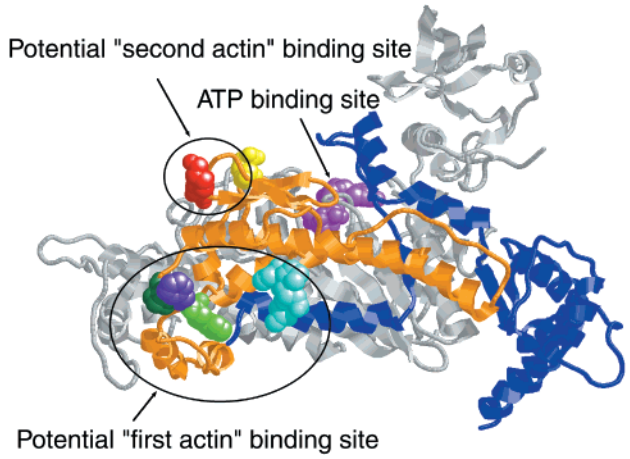

FIGURE 1: Potential actin-binding ionic and hydrophobic surface loops of smooth muscle myosin. The crystal structure of the smooth muscle myosin motor domain−essential light chain construct with MgADP·AlF_4 is adapted from ref *3*. Backbone atoms of the sequences of residues 467−634 and 656−821 of the heavy chain are colored orange and blue, respectively. Potential actin-binding residues Lys-576−Lys-578 (red), Glu-473 (yellow), Trp-546 (light green), Phe-547 (purple), Pro-548 (dark green), and Thr-532/Asn-533/Pro-534/Pro-535 (cyan) are shown as space-filled balls. The analogue MgADP·AlF_4, simulating MgADP·P_i, is shown as space-filled balls in magenta. The Lys-576−Lys-578 fragment lies in a small loop for binding one actin monomer (termed the second actin in the text). Glu-473 is close to the small actin-binding loop. The hydrophobic Trp-546/Phe-547/Pro-548 triplet are exposed near the 50 kDa−20 kDa junction. These residues have been proposed as a potential binding site for the adjacent actin monomer (termed the first actin in the text). The Thr-532/Asn-533/Pro-534/Pro-535 sequence is also exposed in the first actin binding region as a surface loop.

Only in the first case would the test truly confirm the inference. But there is another reason for preferring functional testing over just the inference: Comparison of two crystallographic models may suggest the location of possible mutual contacts (*2*, *4*, *5*), but cannot suggest when in time these occur in relation to one another. To the extent that kinetic models fit the data, they do commit themselves to time dependence. So, without intending to minimize the pioneering contributions of crystallographic comparison, we undertake here the corresponding functional tests, and find it possible, as well, to contribute information about the time sequence in which contacts are made.

MATERIALS AND METHODS

Protein Preparations. F-Actin was purified from rabbit skeletal muscle by the method of Spudich and Watt (*6*). Myosin light chain kinase was prepared from chicken gizzard as described by Adelstein and Klee (*7*). Bovine testis calmodulin was purified by the method of Yazawa et al. (*8*).

Expression of Recombinant HMMs.[1] Wild-type chicken gizzard HMM was prepared as previously described (*9*, *10*). Eleven mutant HMMs, viz., K576A/K578A, E473K, W546A, W546S, F547A, F547H, P548A, P548G, P548R, TNPP(532−535)M, and TNPP(532−535)K, were produced by the same method that was used to prepare wild-type HMM, except that differently mutagenized MGH-6 derivatives were used. MGH-6 is a cDNA encoding the N-terminal half (Met-1−Glu-729) of the chicken gizzard HMM heavy chain (*11*). GMH-6 was mutagenized by the method of Kunkel et al. (*12*) with the following oligonucleotides (the underlined nucleotides indicate imposed mutations): 5′-TCCAGAAGTCCAAACAACTCGCCGATGCCACTGAGTTCTGCATACTGCAC-3′ to replace Lys-576 and Lys-578 with two Ala residues, 5′-GCTGGATTTGAGATTTTTAAGATCAATTTCTTTC-3′ to replace Glu-473 with Lys, 5′-CTGCTGGATGAAGAGTGCGCCTTTCCCAAAGCTACTGAC-3′ and 5′-GGATGAAGAGTGCTCGTTTCCCAAAGC-3′ to replace Trp-546 with Ala and Ser, respectively, 5′-GGATGAAGAGTGCTGGGCTCCCAAAGCTACTGAC-3′ and 5′-GGATGAAGAGTGCTGGCACCCCAAAGCTACTGACAC-3′ to replace Phe-547 with Ala and His, respectively, 5′-GAAGAGTGCTGGTTTGCCAAAGCTACTGAC-3′, 5′-GAAGAGTGCTGGTTTGGCAAAGCTACTGACACT-3′, and 5′-GAGTGCTGGTTTCGCAAAGCTACTGAC-3′ to replace Pro-548 with Ala, Gly, and Arg, respectively, 5′-GCATTGAGCTAATTGAAAGACCTATGGGTGTCCTAGCTCTGCTGGATG-3′ to replace the Thr-532/Asn-533/Pro-534/Pro-535 sequence with a single Met, and 5′-GCTAATTGAAAGACCTAAGGGTGTCCTAGCTC-3′ to further replace this Met with Lys.

To obtain various transfer vectors encoding full-length mutant HMM heavy chains, each *Nco*I−*Eco*RI fragment of the 11 mutagenized MGH-6 derivatives (the N-terminal half) was inserted into a baculovirus vector pAcC4 containing the C-terminal (Phe-730−Thr-1318) half of the HMM heavy chain. Both the transfer vector and linearized *Autographa californica* baculovirus DNA were simultaneously transfected into Sf9 (*Spodoptera frugiperda*) insect cells following the manufacturer's protocol (Invitrogen Co., San Diego, CA) to produce recombinant viruses. Recombinant viruses were isolated by plaque formation as described by Summers and Smith (*13*). Both the HMM heavy chain-containing virus and the virus containing both light chains (for each virus, the ratio of virus to cell was 8) were simultaneously applied to Sf9 cells to produce HMM proteins. Purification of expressed HMMs was carried out as described by Onishi et al. (*10*).

For the in vitro motility assay, wild-type chicken gizzard HMM with His (at its N-terminal end) and myc (at its C-terminal end) tags and similarly tagged mutant HMMs, viz., K576A/K578A, E473K, W548A, and TNPP(532−535)M, were prepared as described by Kojima et al. (*14*). Recombinant bacmid DNAs for expressing the tagged HMM heavy chains were produced by transforming DH10Bac *Escherichia coli* cells with pFastBacHTa plasmids containing the full-length sequence of the HMM heavy chain DNAs according to the manufacturer's protocol (Life Technologies, Rockville, MD). Viruses were produced by transfecting Sf9 cells with recombinant bacmid DNAs and used to produce HMM proteins. Tagged HMMs were purified by actin−HMM precipitation and then by affinity chromatography using Ni−NTA agarose (Quiagen, Valencia, CA).

Gel Electrophoresis and Autoradiography. SDS−PAGE was carried out as described by Laemmli (*15*). Phosphorylation of the regulatory light chain of HMMs was performed as described previously (*9*). Samples were subjected to SDS−PAGE, and ^{32}P bound to the regulatory light chain was detected by exposing the gel to a BAS SR2025 imaging plate and scanning the plate with a BAS 5000 imaging analyzer (Fuji, Kanazawa, Japan).

[1] Abbreviation: HMM, heavy meromyosin.

Negative Staining. Wild-type and mutant HMMs (16 μg/mL) were mixed with rabbit skeletal muscle F-actin (2 μg/mL). The decorated actin filaments were stained with 4% uranyl acetate in distilled water and observed with a 2000FX electron microscope (JEOL, Tokyo, Japan) operated at 80 kV.

ATPase Assays. The basal ATPase activity was measured at 25 °C in an assay medium containing 0.24 mg/mL HMM, 2 mM $MgCl_2$, 20 mM Tris-HCl (pH 7.5), 0.5 mM dithiothreitol, and 0.5 mM ATP with 0.8 mM EGTA (for the activity of unphosphorylated HMM) or with 4 μg/mL chicken gizzard myosin light chain kinase, 1 μg/mL bovine testis calmodulin, and 0.05 mM $CaCl_2$ (for the activity of phosphorylated HMM). KCl concentrations were varied from 0.04 to 0.6 M. Phosphorylation was performed by preincubating HMMs for 15 min at 25 °C in 40 mM KCl in the presence of ATP, myosin light chain kinase, calmodulin, and $CaCl_2$. The ATPase assay was started by adjusting the KCl concentration to the desired level for the assay.

The actin-activated ATPase activity was measured at 25 °C as a function of actin concentration in an assay medium containing 40 mM KCl, 2 mM $MgCl_2$, 20 mM Tris-HCl (pH 7.5), 0.5 mM dithiothreitol, and 1 mM ATP with 0.8 mM EGTA (for the activity of unphosphorylated HMM) or with 4 μg/mL chicken gizzard myosin light chain kinase, 1 μg/mL bovine testis calmodulin, and 0.05 mM $CaCl_2$ (for the activity of phosphorylated HMM). Adding perchloric acid at a final concentration of 0.3 M stopped the ATPase reactions. The amount of released phosphate was measured colorimetrically using the malachite green reagent (*16*, *17*).

In Vitro Motility Assay. The motility assay was performed as described previously (*14*). Briefly, an anti-c-myc monoclonal antibody (clone 9E10; Genosys Biotechnologies) was adsorbed to a nitrocellulose-coated glass surface in a flow cell, created by a nitrocellulose-coated 24 mm × 36 mm coverslip and an 18 mm × 18 mm coverslip. HMM with a myc tag was infused into the flow cell and allowed to bind via anti-c-myc antibodies to the nitrocellulose-coated glass surface. Bound HMM was phosphorylated by incubating it with myosin light chain kinase, calmodulin, and $CaCl_2$. Rhodamine-phalloidine-labeled F-actin was infused into the flow cell, and the sliding movement of fluorescently labeled actin filaments in the presence of ATP was observed with an IX70 inverted microscope (Olympus) equipped with epifluorescence optics and tetramethyl rhodamine filters. Fluorescent images were detected with a C2400 SIT camera (Hamamatsu Photonics) and recorded with an Hi-8 videorecorder (Sony).

RESULTS

Purification of Active Mutant HMMs. All of the mutants, viz., K576A/K578A, E473K, W546A, W546S, F547A, F547H, P548A, P548G, P548R, TNPP(532−535)M, and TNPP(532−535)K, of smooth muscle HMM were isolated by the same protocol used for wild-type HMM (*9*, *10*). The yields of these mutants were not significantly different from that of the wild type. This isolation method is based on myosin functions, viz., coprecipitation with actin and ATP-dependent release from actin. So, these mutants appeared to interact with actin in an ATP-dependent manner, even though these mutations occurred in the actin-binding region. SDS−PAGE indicated that all of the HMM preparations were composed of a 140 kDa HMM heavy chain and an essential light chain (17 kDa) and a regulatory light chain (20 kDa) (data not shown). We also tested whether these mutants are phosphorylatable. The extent of regulatory light chain phosphorylation was analyzed quantitatively by using [γ-^{32}P]-ATP. The amount relative to that of the wild type was determined to be between 0.94 and 1.05 with all of the mutants. This result suggests that these mutants, as well as the wild type, could be fully phosphorylated by myosin light chain kinase, calmodulin, and Ca^{2+}.

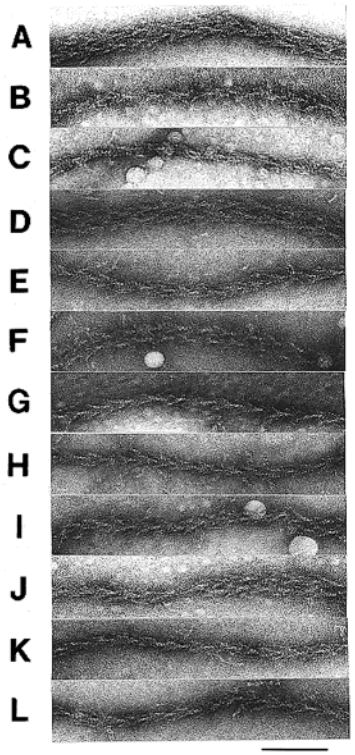

FIGURE 2: Electron micrographs of actin filaments decorated by wild-type and various mutant HMMs. Panels A−L correspond to wild-type, K576A/K578A, E473K, W546A, W546S, F547A, F547H, P548A, P548G, P548R, TNPP(632−535)M, and TNPP-(532−535)K HMM, respectively. These HMMs were mixed with F-actin at a molar ratio of 1:2 to form rigor complexes. The bar is 100 nm long.

Actin Filaments Decorated with Mutant HMMs. To examine whether the mutant HMMs can form typical "rigor" complexes with actin, we mixed each of the mutant HMMs with actin filaments in the absence of ATP. Electron microscope observations indicate that all of the mutant HMMs (Figure 2B−L) decorate actin filaments with an arrowhead appearance similar to that observed with wild-type HMM (Figure 2A). This result suggests that these mutant HMMs can fully decorate actin filaments and probably interact with actin filaments in a stereospecific manner, as in the rigor complexing of wild-type HMM and actin.

Activity of Mutant HMMs. Previous studies (*18*−*20*) have established that wild-type myosin and HMM undergo interesting structural transitions that are correlated with their Mg-ATPase activities. Specifically, in HMM, the sedimentation coefficient, S_{20}, is a tight linear function of the salt concentration (*20*). It is for this reason that variation of activity with salt concentration, e.g., Figure 3, mirrors variation of the structural transition (conversion from the 9S,

Table 1: Intrinsic Mg-ATPase Activities (s^{-1} $head^{-1}$) of Wild-Type HMM and 11 Mutant HMMs[a]

	phosphorylated HMM		unphosphorylated HMM	
	0.08 M KCl	0.45 M KCl	0.08 M KCl	0.45 M KCl
WT	0.014 ± 0.002 (4)	0.012 ± 0.002 (3)	0.0035 ± 0.0002 (4)	0.011 ± 0.001 (7)
K576A/K578A	0.012 ± 0.001 (4)	0.012 ± 0.001 (4)	0.0035 ± 0.0004 (4)	0.010 ± 0.001 (4)
E473K	0.020 ± 0.001 (4)	0.016 ± 0.001 (4)	0.0053 ± 0.0002 (4)	0.013 ± 0.001 (6)
W546A	0.023 (1)	0.017 (1)	0.0073 (1)	0.015 (1)
W546S	0.025 ± 0.002 (2)	0.019 ± 0.001 (2)	0.0082 ± 0.0001 (2)	0.015 ± 0.001 (2)
F547A	0.014 (1)	0.012 (1)	0.0028 (1)	0.010 (1)
F547H	0.014 ± 0.001 (2)	0.013 ± 0.001 (2)	0.0031 ± 0.0002 (2)	0.011 ± 0.001 (2)
P548A	0.014 (1)	0.013 (1)	0.0030 (1)	0.010 (1)
P548G	0.020 ± 0.002 (2)	0.018 ± 0.002 (2)	0.0043 ± 0.0004 (2)	0.014 ± 0.001 (2)
P548R	0.011 (1)	0.014 (1)	0.0023 (1)	0.011 (1)
TNPP(532−535)M	0.013 ± 0.001 (2)	0.014 ± 0.001 (2)	0.0029 ± 0.0002 (2)	0.011 ± 0.001 (2)
TNPP(532−535)K	0.016 (1)	0.011 (1)	0.030 (1)	0.010 (1)

[a] Assay conditions were the same as those described in the legend of Figure 3, except the KCl concentrations were 0.08 and 0.45 M. The activities are reported as the average and the standard error, when the experiment was performed more than one time; the number of times is in parentheses.

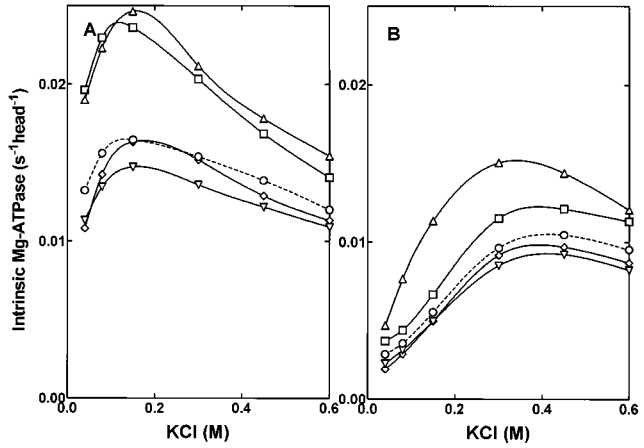

FIGURE 3: Mg-ATPase activities of wild-type HMM and four mutant HMMs as a function of KCl concentration. Assay conditions included wild-type (○), K576A/K578A (▽), E473K (□), W546S (△), and F547H (◇) HMMs (each at 0.24 mg/mL), 2 mM $MgCl_2$, 20 mM Tris-HCl (pH 7.5), 0.5 mM dithiothreitol, and 0.5 mM ATP with 4 μg/mL myosin light chain kinase, 1 μg/mL calmodulin, and 0.05 mM $CaCl_2$ or with 0.8 mM EGTA. (A) Phosphorylated HMM. Before the ATPase assay, HMM was phosphorylated by incubating it for 15 min at 25 °C in the low-salt medium (40 mM KCl) with myosin light chain kinase (MLCK), calmodulin, and $CaCl_2$. Each assay was started by adjusting the KCl concentration to an appropriate value. (B) Unphosphorylated HMM. EGTA was added to the medium instead of MLCK, calmodulin, and $CaCl_2$.

"bent", state to the 7.5 S, "straight", state) with salt concentration. It was also established in these previous studies that, as a function of salt concentration, plots of Mg-ATPase activity, or plots of sedimentation velocity, are translated to higher salt concentrations when the system is changed from a phosphorylated to a nonphosphorylated condition. The wild-type behavior just described is illustrated by the curves through the circles in panels A and B of Figure 3. It is notable that essentially the same dependence on salt concentration is exhibited by the activities of four mutant systems, K576A/K578A, E473K, W546S, and F547H, illustrated in the same figure. Many similar illustrations are given in Table 1, for the various systems studied here, such as the ATPase activities at two "standard" KCl concentrations (0.08 and 0.45 M), for both unphosphorylated and phosphorylated systems. These observations suggest that all the mutants, like the wild type, undergo the characteristic smooth muscle transition; conversely, there is no indication that mutations in the actin-binding region of HMM play a significant role in the transition.

Actin Activation of Mutant HMM ATPases. As mentioned in the introductory section, Lys-576 and Lys-578 map in the loop of HMM at which the second actin binds. Glu-473 is near this loop. To investigate the influence of these charged residues, they were mutated, and the actin-activated ATPase activities of the resulting HMMs were individually measured, in both the phosphorylated and unphosphorylated states, as a function of actin concentration (Figure 4A,B). From the fitting of the phosphorylated activities of the two mutants and the wild type to the simplified equation $V = V_{max}/(1 + K_{app}/[actin])$, the V_{max} and K_{app} parameters were obtained (Table 2). Here, V is the actin-activated rate of ATP hydrolysis, V_{max} the maximum rate, and K_{app} the apparent dissociation constant of acto-HMM. For the wild type, we obtain values of 2.0 s^{-1} $head^{-1}$ and 0.12 mM for V_{max} and K_{app}, respectively. In K576A/K578A, K_{app} is 3.5 times greater, and in E473K, it is 5 times smaller. A natural inference is that, in the wild type, the positively charged lysine residues are attracting negatively charged residues of actin, and that the neighboring negatively charged glutamate repels the same residues of actin. On the other hand, the V_{max} values of the two mutants are similar to that of the wild type, suggesting that the interaction of these residues with actin is unimportant in determining the actin-activated ATPase rate during the rate-limiting step.

As also described in the introductory section, the Trp-546/Phe-547/Pro-548 triplet and the Thr-532/Asn-533/Pro-534/Pro-535 loop were proposed as sites of interaction with the first actin. To examine the involvement of the two hydrophobic surface loops of HMM in the interaction with actin during the ATPase process, we studied the effect of actin concentration on the actin-activated ATPase activity of mutant HMMs in which each component of the triplet was replaced with other amino acids (Figure 5A,B) and in which the proline-rich loop was replaced with a single Met or Lys residue (Figure 6A,B). Figure 5A shows that in the phosphorylated state, each of the mutants of the triplet has a greatly reduced activity compared to that of the wild type. This strongly suggests that this potential actin-binding triplet is involved in the hydrophobic interaction with actin. Since F547A and F547H mutants had practically no actin activation

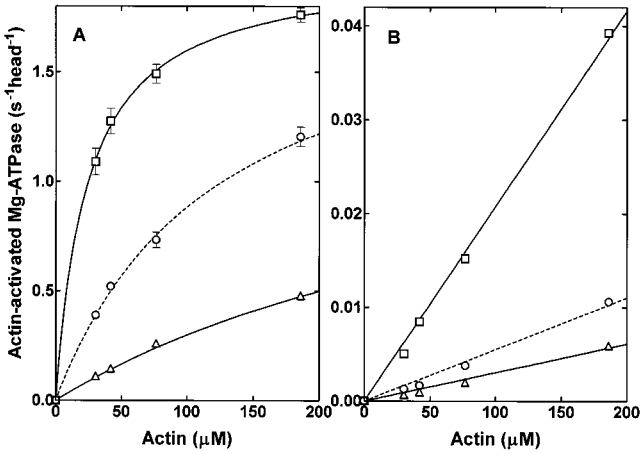

FIGURE 4: Actin-activated Mg-ATPase activities of wild-type HMM and two mutant HMMs at the second actin binding site as a function of actin concentration. Assays were carried out by incubating wild-type (○), K576A/K578A (△), and E473K (□) HMMs at 25 °C in the medium containing various concentrations of actin, 40 mM KCl, 2 mM $MgCl_2$, 20 mM Tris-HCl (pH 7.5), 0.5 mM dithiothreitol, and 1 mM ATP. (A) Phosphorylated HMM. The concentration of HMMs was 0.03−0.06 mg/mL. Myosin light chain kinase (4 μg/mL), calmodulin (1 μg/mL), and $CaCl_2$ (0.05 mM) were added to the assay medium to phosphorylate the regulatory light chain. (B) Unphosphorylated HMM. The concentration of HMMs was 0.24 mg/mL. EGTA was added to final concentration of 0.8 mM, instead of MLCK, calmodulin, and $CaCl_2$. The ATPase activities of HMM alone and actin alone were subtracted from each measured value to estimate actin-activated ATPase activity. Error bars show the standard deviation of the data when the measurements are carried out more than once. The measurements for each of the mutants are summarized in Table 2. For the phosphorylated HMMs, curves were fitted to the data sets using the equation $V = V_{max}/(1 + K_{app}/[actin])$. Straight lines were fitted to the data sets to define V_{max}/K_{app} for the unphosphorylated HMM. V_{max}/K_{app}, V_{max}, and K_{app} values are summarized in Table 2.

activity, their V_{max} and K_{app} values could not be determined. The ATPase activities of W546A, W546S, P548A, P548G, and P548R mutants increased with increasing actin concentrations. We roughly estimate V_{max} and K_{app} values for these mutants by using the same equation as in Figure 4A (Table 2). V_{max} was significantly reduced and ranges from $^2/_{100}$ of the wild-type rate for the P548G mutant to $^6/_{100}$ of the wild-type rate for the W546A mutant. On the other hand, K_{app} was not so significantly changed (1.5−4.5-fold greater than that of the wild type) by these mutations. Therefore, it is suggested that the reduced level of activation is mainly caused by the slowed rate-limiting step of the actin-activated ATPase reaction. The weak binding of these mutants to actin during the ATPase reaction also suggests that the slowed step is likely to occur prior to the transition from the weakly to the strongly bound state with actin.

The actin-activated ATPase activity of the phosphorylated TNPP(532−535)M mutant was increased compared to that of the wild type, whereas that of phosphorylated TNPP(532−535)K mutant decreased (Figure 6A). When these curves were fitted to the equation $V = V_{max}/(1 + K_{app}/[actin])$, where V_{max} and K_{app} were estimated to be 3.9 s^{-1} $head^{-1}$ and 0.1 mM, respectively, for TNPP(532−535)M and 0.85 s^{-1} $head^{-1}$ and 0.048 mM, respectively, for TNPP(532−535)K (Table 2). Therefore, V_{max} values of TNPP(532−535)M and TNPP(532−535)K were about 2-fold greater than and $^1/_2$ of that of the wild type, respectively. We thus suggest that in contrast to a small loop including the Lys-576−Lys-578 sequence, the interaction of this Pro-rich loop with actin is important in determining the actin-activated ATPase rate during the rate-limiting step.

As the actin-activated ATPase activities of the unphosphorylated form of the wild type and mutants exhibited a linear relation with respect to the actin concentration (Figures 4B, 5B, and 6B), their V_{max} and K_{app} values could not be determined independently. To characterize the unphosphorylated form of the mutants, we used the apparent second-order rate constant V_{max}/K_{app} estimated from the slope of their activities versus actin concentration. In K576A/K578A, E473K, W546A, W546S, P548A, P548G, P548R, TNPP(532−535)M, and TNPP(532−535)K mutants, V_{max}/K_{app} was much smaller for their unphosphorylated form than for their phosphorylated form, suggesting that these mutations do not cause a drastic loss in the level of regulation by phosphorylation (Table 2). However, it was impossible to discover whether actin activation of F547A and F547H mutants occurred in a phosphorylation-dependent manner, because their actin-activated ATPase activities were very small for both phosphorylated and unphosphorylated forms.

In Vitro Motility of Mutant HMMs. To examine whether the actin-activated ATPase activity is coupled to the myosin motor function, motility assays of the wild type and some mutant HMMs were carried out. When the regulatory light chain was phosphorylated, wild-type HMM moved actin filaments at an average of 0.41 μm/s (Figure 7). Under the same condition, K476A/K578A and E473K HMMs supported uniform movement of actin filaments at roughly the same velocity as that of the wild type (0.38 μm/s for K576A/K578A and 0.39 μm/s for E473K). As shown in Table 2, V_{max} of these mutants was similar to that of the wild type, but their K_{app} values were different from the wild-type value. Thus, under our assay conditions, the velocity of actin movement correlates with V_{max} values of the actin-activated ATPase activity.

W548A could not support filament movement (Figure 7). This is reasonable, because this mutant had a very limited V_{max} of the actin-activated ATPase activity (Table 2). To examine the ability of this mutant to retard actin movement driven by wild-type HMM, we also performed a motility assay with equal concentrations of wild-type and W548A mutant HMMs. Actin filament moved at a velocity of 0.38 μm/s (Figure 7). The presence of W548A HMM did not slow the movement of actin filaments. This result suggests that W548A is in a weakly bound state for actin, thus resulting in no significant retardation in the movement of actin filaments driven by wild-type HMM.

As we have demonstrated, V_{max} of the TNPP(532−535)M mutant was about 2-fold greater than that of the wild type (Table 2). If the velocity of actin filament movement is proportional to the V_{max} of the actin-activated ATPase activity, then this mutant is expected to move actin filaments at a higher velocity. To determine if this is correct, we measured the velocity of actin filaments moved by this mutant. As expected, filament movement (∼0.6 μm/s) was about 50% faster than that of the wild type (Figure 7).

DISCUSSION

To understand the importance of particular residues in myosin function, we engineered point mutations in the

Table 2: Maximum Velocities (V_{max}), Apparent Dissociation Constants for Actin (K_{app}), and Apparent Second-Order Rate Constants (V_{max}/K_{app}) of Actin-Activated Mg-ATPase Activities of Wild-Type HMM and 11 Mutant HMMs[a]

	phosphorylated HMM			unphosphorylated HMM
	V_{max} (s^{-1} $head^{-1}$)	K_{app} (mM)	V_{max}/K_{app} (s^{-1} $head^{-1}$ mM^{-1})	V_{max}/K_{app} (s^{-1} $head^{-1}$ mM^{-1})
WT	2.0 ± 0.1	0.12 ± 0.02	15 (6)	0.06 (1)
K576A/K578A	1.5 ± 0.1	0.40 ± 0.04	3.8 (5)	0.03 (1)
E473K	2.0 ± 0.1	0.024 ± 0.003	83 (5)	0.21 (2)
W546A	0.12 ± 0.01	0.18 ± 0.03	0.67 (3)	0.02 (1)
W546S	0.07	0.18	0.39 (1)	<0.01 (1)
F547A			<0.01 (1)	<0.01 (1)
F547H			<0.01 (1)	<0.01 (1)
P548A	0.07	0.28	0.25 (1)	<0.01 (1)
P548G	0.043 ± 0.007	0.50 ± 0.10	0.09 (7)	<0.01 (3)
P548R	0.05	0.26	0.19 (1)	<0.01 (1)
TNPP(532−535)M	3.9	0.10	39 (1)	0.12 (1)
TNPP(532−535)K	0.85 ± 0.03	0.048 ± 0.04	18 (2)	0.04 (2)

[a] Assay conditions were the same as those described in the legend of Figure 4, except various mutant HMMs were used. The standard error is given for each mean value of V_{max} and K_{app}, when the experiment was performed more than one time; the number of times is in parentheses.

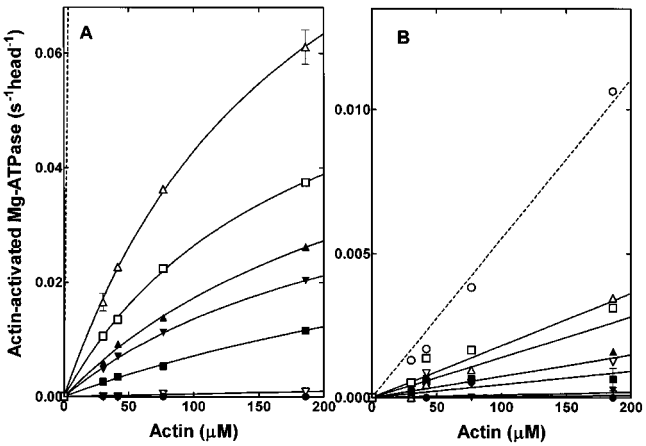

FIGURE 5: Actin-activated Mg-ATPase activities of seven mutant HMMs at the hydrophobic triplet as a function of actin concentration. Assay conditions were the same as those described in the legend of Figure 4, except that wild-type (○), W546A (△), W546S (□), F547A (▽), F547H (●), P548A (▲), P548G (■), and P548R (▼) HMMs were used. Concentrations of the phosphorylated and unphosphorylated forms of HMMs were 0.14−0.24 mg/mL.

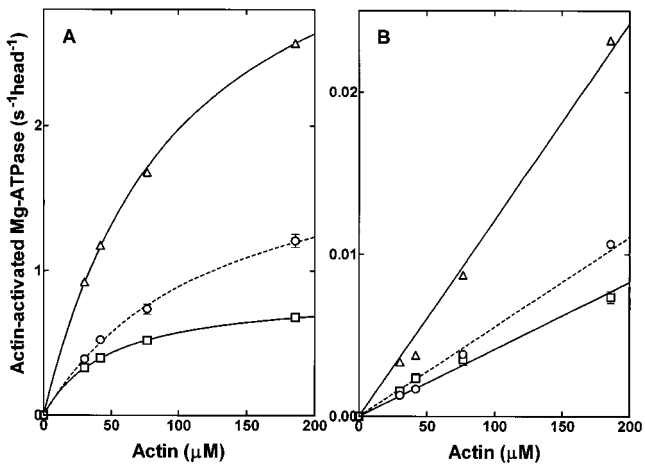

FIGURE 6: Actin-activated Mg-ATPase activities of two mutant HMMs at the Pro-rich loop as a function of actin concentration. Assay conditions were the same as those described in the legend of Figure 4, except that wild-type (○), TNPP(532−535)M (△), and TNPP(532−535)K (□) HMMs were used. Concentrations were 0.03−0.06 mg/mL for the phosphorylated form and 0.24 mg/mL for the unphosphorylated form.

presumed actin-binding region of the smooth muscle HMM heavy chain. These mutations did not affect functional features such as light chain phosphorylation or dependence on salt concentration in the absence of actin, indicating that the intrinsic catalytic site in these mutants remained normal. For example, all of the mutants decorated actin filaments just as did wild-type HMM (Figure 2), and the decoration was reversible upon adding ATP. This behavior suggests that although the mutation of one or two residues in their actin-binding regions may slightly weaken their affinities for actin, the mutants continue to attach to actin in a stereospecific manner. However, these mutants do have certain defects related to their interactions with actin, and these are manifested in their ATPase activities. Specifically, kinetic analysis revealed that these defects were different depending on where in the actin-binding area they were made.

Second Actin Binding Site. When we fit our two-parameter (K_{app} and V_{max}) model to the ATPase data generated by K576A/K578A, we find that this mutant is characterized by an increased K_{app}, but an unchanged V_{max}, and an unchanged motility (Figure 4 and Table 2). So, if we grant the validity of the model, we suppose that this small cationic loop, in the wild type, engages in an "early", non-rate-limiting, attachment to actin, but not in a rate-limiting "late" event, such as the "leaving" reaction or the power stroke.

From fitting together chicken skeletal myosin subfragment 1 and rabbit skeletal actin crystal structures, Rayment et al. (*2*) postulated that Lys-572 and Lys-574 of S1 (corresponding to residues 576 and 578 in the chicken gizzard myosin sequence) can interact with the charged pair of the "second actin" (Glu-99 and Glu-100). Our results are consistent with this idea. Moreover, from analyzing the actin mutant E99A/E100A, Miller and Reisler (*21*) suggested that these residues are important for the binding of myosin with actin. They also found that this mutation did not affect motility. Their actin, and our HMM, mutants exhibited similar defects. Their finding also supports the idea that Lys-576 and Lys-578 of smooth muscle HMM interact directly with the charged pair of actin (Glu-99 and Glu-100).

Previous reports relate to our observations. Using *Dictyostelium* myosin subfragment 1, Giese and Spudich (*22*)

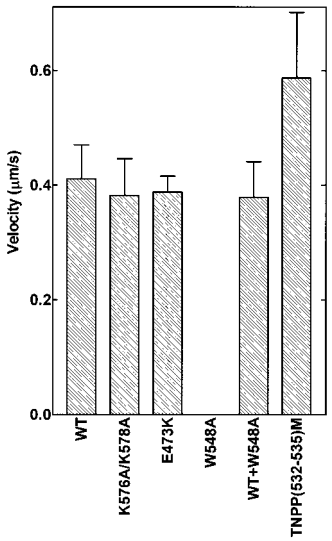

FIGURE 7: Actin sliding velocities of wild-type and mutant HMMs measured by in vitro motility assays. Motility assays were carried out at 30 °C under the conditions described in Materials and Methods. The mean sliding velocity produced by wild-type HMM, by each of mutant HMMs, or by mixtures of equal amounts of wild-type and mutant HMMs is shown. Error bars show the standard deviation of velocities of moving actin filaments.

introduced the mutation R562L, and reported that the resulting reduced level of actin activation correlated with a reduced V_{max}. On the other hand, Dijk et al. (*23*), who constructed chimeras in which the small loop sequence (KEK) was introduced into *Dictyostelium* beginning with Lys-565, reported a 4−6-fold increase in affinity for actin and an unchanged V_{max}. The behavior following our present mutation (from KEK to AEA, with no change in V_{max}, but with an increase in K_{app}) seems entirely consistent with the behavior described by Dijk et al. (from K to KEK, with no change in V_{max}, but with a decrease in V_{max}), and out of step with that described by Giese and Spudich (from R to L, with a decrease in V_{max}). However, it must be noted that here and in ref *23* the residue charge was varied at the small loop position, but in ref *22* it was varied at a position three residues downstream from the small loop position.

A similar interpretation can be applied to our results with E473K. Glu-473 is close to the Lys-576−Lys-578 sequence of the small (second) actin-binding loop. It is also connected to the nucleotide-binding loop switch II by a stiff β-strand. These features previously led us to speculate that Glu-473 might be key in communication between the actin binding site and the ATPase active site. The simplest interpretation of the behavior of E473K, however, does not support the speculation. One would expect that an inversion of charge in the transmission line would completely confuse the transmission, yet V_{max} remains unchanged by the mutation, as does the ability to move actin filaments at normal speed. Inversion to a positive charge at 473 could conceivably paralyze the transmission in the "on" position; this could happen without being rate-limiting, but at best, the original speculation remains unsubstantiated.

Hydrophobic Triplet. Previously, we reported that the W546S/F547H double mutant of smooth muscle HMM has an impaired actin-activated ATPase activity (*24*). In *Dictyostelium* myosin, Giese and Spudich (*22*) found that the P536R mutant (which corresponds to the chicken gizzard myosin residue Pro-548) has a reduced level of actin activation. These studies suggested that all of the Trp-546, Phe-547, and Pro-548 residues might be important participants in the hydrophobic actin−myosin interaction. Here, we have produced several single substitutions at W546, F547, and P548 residues and found that all of the mutants are strongly impaired in their actin-activated ATPase activities.

Amino acid substitutions made within the hydrophobic triplet gave results completely different from those obtained from HMMs with mutations in the second actin binding site. We have found that the reduced level of actin activation observed in the W546A, W546S, P548A, P548G, and P548R mutants is primarily due to a decreased V_{max} (Figure 5 and Table 2). Thus, this reduction probably results from a rate change in a step that occurs after actin is bound. The hydrophobic triplet may be important for product release from the actin−HMM complex or in the transition from the a weak- to strong-binding state. We have also found that the W548A mutant does not support the movement of actin filaments, but this mutant does not slow the velocity of filament movement when mixed with the wild type at a molar ratio of 1:1 (Figure 7). This result can be interpreted by assuming that its affinity for actin is lower than that of the wild type so that in competition with the wild type this mutant is excluded and the observed movement of actin filaments is that of the wild type. In fact, we found that the K_{app} of W548A was somewhat larger than that of the wild type (Table 2). Thus, we propose that the W548A mutation disables the formation of the strongly bound state in the presence of ATP, although it retains the ability to form the "rigor" strong-binding complex with actin in the absence of ATP.

The level of actin activation of all of our mutants within the hydrophobic triplet was greatly reduced compared to that of the wild type (Figure 5). Therefore, it may be that bulky side chains are required for high-level actin activation. Sequence alignment in the myosin II family suggests that the first residue of the hydrophobic triplet can be substituted with some bulky hydrophobic amino acids, such as Met in skeletal and cardiac sequences and Val in the *Dictyostelium* sequence, but that the second and third residues are highly conserved. These bulky side chains probably create an interface between HMM and actin residues that fits well.

Proline-Rich Loop. As the Pro-rich loop of smooth muscle myosin is substituted with a single Met residue in the skeletal muscle sequence (*25*), this loop may not be absolutely necessary for myosin function. We propose that this part of the actin-binding region does not have strong structural restrictions. We have shown that the level of actin activation of the ATPase activity of the chimera HMM, in which this loop is replaced with a sequence derived from skeletal myosin, is about 2-fold greater than that of wild-type HMM (Figure 6). The increased level of activation is correlated with an increase in V_{max} (Table 2) and an increase in the velocity of the movement of actin filaments (Figure 7). Therefore, the slow contraction of smooth muscle may be explained partially by the presence of this proline-rich surface loop. Since the level of actin activation of the chimeric ATPase activity was reduced by replacing the Met with Lys, it is obvious that this Met residue can participate in the hydrophobic interaction between actin and myosin in the chimeric system.

Roles of Ionic and Hydrophobic Residues. Various HMM mutations in the actin-binding region suggest that ionic and hydrophobic surface loops have distinct roles in motor function. Our results show the importance of the hydrophobic triplet in the actin activation of HMM ATPase. The significant reduction of the mutant V_{max} compared to the same parameter for the wild type suggests that in the wild-type behavior the parameter expresses the "late event" product release incident to formation of the strongly bound state. The power stroke is thought to be a late event in the actin-activated ATPase. So, our results fit well with the ideas of Zhao and Kawai (*26*) and Geeves and Conibear (*27*) in that forming the hydrophobic interaction between actin and myosin is followed by transition from the weakly to the strongly bound state, and that this hydrophobic interaction is central to the contractile function being the end state of the power stroke. Moreover, our finding that the W548A mutant does not slow the rate of movement of actin filaments when mixed with the wild type at a molar ratio of 1:1 in an in vitro motility assay is consistent with the model in which the hydrophobic interaction of the triplet with actin is important for the formation of the strongly bound state with actin.

On the basis of the crystallographic study, Rayment et al. (*1*) predicted that the initial recognition between myosin and actin occurred via ionic interactions of lysines in the 50 kDa−20 kDa junction of myosin with N-terminal negatively charged residues of actin. Rovner et al. (*28*) studied a chimeric smooth muscle HMM with a sequence derived from the 50 kDa−20 kDa junction of skeletal myosin. Their chimera exhibited a reduced K_{app} for actin, but there was little effect on the V_{max} of actin-activated ATPase. This study confirms that positively charged residues in the second actin binding loop of smooth muscle HMM are important for the binding affinity for actin during the ATPase reaction. Therefore, in the smooth muscle myosin system, the ionic residues in both the 50 kDa−20 kDa surface loop and the second actin binding surface loop seem to be involved in the weak binding affinity for actin before actin is strongly bound.

In summary, various mutations in the actin-binding region of smooth muscle HMM appeared not to perturb the intrinsic ATPase activity, but affected greatly the actin-activated ATPase activity. From the steady-state analysis of the actin-activated ATPase activity of these mutants, defects could be grouped around K_{app} or V_{max}, thus identifying them as either early or late event in myosin ATPase hydrolysis. This finding allows us to propose that some HMM residues are involved in the association of HMM with actin, whereas other residues have important roles in the product release.

ACKNOWLEDGMENT

We thank Mrs. Haruyo Sakamoto for her technical assistance.

REFERENCES

1. Rayment, I., Rypniewski, W. R., Schmidt-Bäse, K., Smith, R., Tomchick, D. R., Benning, M. M., Winkelmann, D. A., Wesenberg, G., and Holden, H. M. (1993) *Science 261*, 50−58.
2. Rayment, I., Holden, H. M., Whittaker, M., Yohn, C. B., Lorenz, M., Holmes, K. C., and Milligan, R. A. (1993) *Science, 261*, 58−65.
3. Dominguez, R., Freyzon, Y., Trybus, K. M., and Cohen, C. (1998) *Cell 94*, 559−571.
4. Kabsch, W., Mannherz, H. G., Suck, D., Pai, E. F., and Holmes, K. C. (1990) *Nature 347*, 37−44.
5. Holmes, K. C., Popp, D., Gebhard, W., and Kabsch, W. (1990) *Nature 347*, 44−49.
6. Spudich, J. A., and Watt, S. (1971) *J. Biol. Chem. 246*, 4866−4871.
7. Adelstein, R. S., and Klee, C. B. (1981) *J. Biol. Chem. 256*, 7501−7509.
8. Yazawa, M., Sakuma, M., and Yagi, K. (1980) *J. Biochem. 87*, 1313−1320.
9. Onishi, H., Maéda, K., Maéda, Y., Inoue, A., and Fujiwara, K. (1995) *Proc. Natl. Acad. Sci. U.S.A. 92*, 704−708.
10. Onishi, H., Morales, M. F., Kojima, S., Katoh, K., and Fujiwara, K. (1997) *Biochemistry 36*, 3767−3772.
11. Yanagisawa, M., Hamada, Y., Katsuragawa, Y., Imamura, M., Mikawa, T., and Masaki, T. (1987) *J. Mol. Biol. 198*, 143−157.
12. Kunkel, T. A., Roberts, J. D., and Zakour, R. A. (1987) *Methods Enzymol. 154*, 367−382.
13. Summers, M. D., and Smith, G. E. (1987) *A Manual of Methods for Baculovirus Vectors and Insect Cell Culture Procedures*, Bulletin 1555, Texas Agricultural Experimental Station, College Station, TX.
14. Kojima, S., Fujiwara, K., and Onishi, H. (1999) *Biochemistry 38*, 11670−11676.
15. Laemmli, U. K. (1970) *Nature 227*, 680−685.
16. Lanzetta, P. A., Alvarez, L. J., Reinach, P. S., and Candia, O. A. (1979) *Anal. Biochem. 100*, 95−97.
17. Ohno, T., and Kodama, T. (1989) in *Muscle Energetics* (Paul, R., and Yamada, K., Eds.) pp 69−73, Alan R. Liss, Inc., New York.
18. Onishi, H. (1982) *J. Biochem. 91*, 157−166.
19. Suzuki, H., Kamata, T., Onishi, H., and Watanabe, S. (1982) *J. Biochem. 91*, 1699−1705.
20. Suzuki, H., Stafford, W. F., III, Slayter, H. S., and Seidel, J. C. (1985) *J. Biol. Chem. 260*, 14810−14817.
21. Miller, C. J., and Reisler, E. (1995) *Biochemistry 34*, 2694−2700.
22. Giese, K. C., and Spudich, J. A. (1997) *Biochemistry 36*, 8465−8473.
23. Dijk, J. V., Furch, M., Lafont, C., Manstein, D. J., and Chaussepied, P. (1999) *Biochemistry 38*, 15078−15085.
24. Onishi, H., Morales, M. F., Katoh, K., and Fujiwara, K. (1995) *Proc. Natl. Acad. Sci. U.S.A. 92*, 11965−11969.
25. Maita, T., Hayashida, M., Tanioka, Y., Komine, Y., and Matsuda, G. (1987) *Proc. Natl. Acad. Sci. U.S.A. 84*, 416−420.
26. Zhao, Y., and Kawai, M. (1995) *Biophys. J. 68*, 332s.
27. Geeves, M. A., and Conibear, P. B. (1995) *Biophys. J. 68*, 194s−201s.
28. Rovner, A. S., Freyzon, Y., and Trybus, K. M. (1995) *J. Biol. Chem. 270*, 30260−30263.

BI0011328